

New Attribute for Determination of Lithology and Brittleness*

Ritesh Kumar Sharma¹ and Satinder Chopra¹

Search and Discovery Article #41368 (2014)

Posted June 9, 2014

*Adapted from extended abstract prepared in conjunction with presentation at CSPG/CSEG/CWLS GeoConvention 2013, (Integration: Geoscience engineering Partnership) Calgary TELUS Convention Centre & ERCB Core Research Centre, Calgary, AB, Canada, 6-12 May 2013, AAPG/CSPG©2014

¹Arcis Seismic Solutions, Calgary, Canada (rsharma@arcis.com)

Abstract

The discrimination of fluid content and lithology in a reservoir is an important characterization that has a bearing on reservoir development and its management. For the unconventional reservoirs, such as shale gas formations, besides other favorable considerations that are expected of them, it is vital that reservoir zones are brittle. Brittle zones fracture better and fracturing of shale gas reservoirs is required for their production. Amongst the different physical parameters that characterize the rocks, Young's modulus (E) is a measure of their brittleness. Attempts are usually made to determine this physical constant from well log data, but such measurements are localized over a small area. For studying lateral variation of brittleness in an area, 3D seismic data needs to be used. Computation of Young's modulus from seismic data requires the availability of density (ρ). The computation of density in turn requires long offset data, which is usually not available. In this study, we propose a new attribute ($E\rho$) in the form of a product of Young's modulus and density. For a brittle rock, both Young's modulus and density are expected to be high, and so the $E\rho$ attribute would exhibit a high value and serve as a brittleness indicator. As well, we demonstrate the usefulness of this new attribute for litho-fluid detection, when it is used in conjunction with the product of bulk modulus and density.

Introduction

The determination of lithology and fluid content distribution in a reservoir is a desirable objective for its characterization and subsequent management. Physical properties such as porosity and permeability make it possible to evaluate a hydrocarbon reservoir. However, the properties that have a direct impact on the relevant elastic constants are bulk modulus, shear modulus, and Young's modulus, amongst others. Bulk modulus (κ) is a measure of a material's resistance to change in volume and is known as incompressibility. It is treated as a porosity indicator. Shear modulus (μ) is measure of rigidity of a rock or resistance to deformation taken in a shear direction and is treated as a lithology indicator. Further, Young's modulus (E), also known as stiffness modulus is a measure of the stiffness of the material of the rock. Historically, based on these physical properties, geoscientists have attempted to delineate the fluid and lithology content of a reservoir. An estimation of the physical properties described above requires P- impedance (I_p), S-impedance (I_s) and density. For computing these prerequisites, prestack inversion of surface seismic data is usually performed. Although, extraction of density from seismic data needs far-offset information, it is also

true that the quality and amplitude fidelity deteriorate significantly at large angles of incidence. Therefore, the computation of density is considered an arduous task.

In the absence of density, efforts have been made for characterization of a reservoir in terms of lithology and fluid content. For this purpose, I_p and I_s are used for litho-fluid discrimination as I_p is sensitive to fluid, whereas I_s is not. Goodway et al (1997) proposed the determination of rock physics parameters such as Lamé's constants (λ and μ) from I_p and I_s and demonstrated that as λ (sensitive to pore fluid) and μ (sensitive to the rigidity of the rock matrix) may be difficult to isolate from seismic data, $\lambda\rho$ and $\mu\rho$, where ρ is density, can be easily determined from I_p and I_s . Besides, these attributes show better discrimination of lithology and fluids in the $\lambda\rho$ - $\mu\rho$ crossplot space. Russell et al (2003) proposed the use of the more generalized fluid term (ρf), instead of just the $\lambda\rho$ attribute. Likewise, Katahara (2001) investigated the application of $\kappa\rho$ attribute using well data, for enhancing the detection of fluid. More recently, Dabagh et al (2011) have shown a comparison of $\kappa\rho$ and $\lambda\rho$, and that $\kappa\rho$ comes out as a superior attribute for fluid detection.

The stiffness of a rock is an important property, especially important for shale gas reservoirs where fracturing is employed for stimulation. Stiffer shales fracture much better than ductile ones and enhance the permeability of those zones. Young's modulus can characterize such stiffer pockets in shales and accordingly Santoso et al (1995) and Banik et al (2010) demonstrated the determination of Young's modulus from seismic data by way of inversion. One limitation of Santoso et al (1995) approach is the requirement of density, which as stated above is difficult to derive from seismic data, unless long offset information is available. Banik et al (2010) alleviate the requirement for density by using the correlation of I_s or I_p and Young's modulus from log data, and using that relationship for computation of Young's modulus.

Considering the importance of a lithology indicator as well as an attribute that could yield information on the brittleness of a reservoir, we propose a new attribute, $E\rho$, which is the product of Young's modulus and density. While $E\rho$ accentuates lithology detection in terms of brittleness, $\kappa\rho$, intensifies fluid detection. $E\rho$ facilitates a new domain, wherein fluid-lithology discrimination can be achieved in a significant way.

Methodology

Young's modulus (E) is the measure of stiffness of a rock and can be defined in terms of bulk modulus (κ) as:

$$E = 3 \kappa (1 - 2\sigma)$$

Where σ is the Poisson's ratio and can be written in terms of P -wave velocity and S -wave velocity as follows:

$$\sigma = \frac{v_p^2 - 2v_s^2}{2v_p^2 - v_s^2}$$

Substitution of this equation into the first one yields:

$$E = \rho v_s^2 \frac{(3v_p^2 - 4v_s^2)}{v_p^2 - v_s^2}$$

If we multiply both sides of the above equation by density and use the relationships $I_p = \rho v_p$ and $I_s = \rho v_s$, the above equation can be written as:

$$E\rho = \mu\rho \frac{3I_p^2 - 4I_s^2}{I_p^2 - I_s^2}$$

Thus, once we compute I_p and I_s using seismic inversion this attribute can be derived directly. Further, above equation can be written as:

$$E\rho = \mu\rho * \alpha$$

Where $\alpha = \frac{(3v_p^2 - 4v_s^2)}{v_p^2 - v_s^2}$

If α turns out to be a positive number then it can be concluded that $E\rho$ is a scaled version of μ and would enhance lithological information. To this end, we consider the following two cases.

Case 1: Brine sand

For brine sand, it is known that $v_p/v_s = 2$ (i.e. $v_p = 2v_s$). Using this it can be shown that

$$E\rho = (8/3)\mu\rho$$

Case 2: Gas sand

For the gas sand case, typically, $v_p/v_s = 1.5$, and so in this case $E\rho$ can be computed as:

$$E\rho = (11/5)\mu\rho$$

We thus conclude from these two cases that whether hydrocarbon is present in a formation or not, $E\rho$ is a scaled version of $\mu\rho$, and so intensifies lithologic information. For a brittle rock, Young's modulus would be high and density would be high too, therefore the product of Young's modulus and density would be high as well and would accentuate the brittleness of the rock.

Examples

We have discussed above the advantage of $E\rho$ for fluid-lithology detection and its implication for fracturing brittle formations. We now demonstrate the computation of $E\rho$ from well log and seismic data, and show its practical importance. In [Figure 1](#), we show a comparison of the $\mu\rho$ and $E\rho$ curves for a well in northern Alberta. Notice, the $E\rho$ curve emphasizes the variation corresponding to lithology change more than in the $\mu\rho$ curve. For ease in interpretation, we segment the input log curves and the results shown in [Figure 2](#) stand out nice and clear.

For implementation of this analysis on seismic data, we considered a gas-impregnated Nordegg member of the Jurassic Fernie formation of the Western Canadian Sedimentary Basin. The Nordegg member of the Fernie formation varies throughout the WCSB. It consists of predominantly brownish, greyish and black shales. These "shales" vary from siliceous rich cherts and dolomites to carbonate rich shale. Due to the complex geology of the reservoir in the Nordegg, differentiating the lithology and fluid content is a challenge. The Nordegg – Montney interface is a regional unconformity, which separates the Jurassic and Triassic strata in the area. The Montney formation is composed of fine-grained siltstone grading to fine grained sandstones, with limited shale content. There is a diagenetic dolomitic overprinting on the siltstones and sandstones. In local areas of the Montney there is a coquina facies made up of bivalves.

Thus, as the first step, simultaneous impedance inversion was run on the pre-conditioned 3D seismic data to obtain P-impedance and S-impedance volumes. Next, these impedance volumes were transformed into $\mu\rho$ and $E\rho$ volumes as discussed above. In [Figures 3 a and b](#), we show segments of vertical sections from the $\mu\rho$ and $E\rho$ volumes respectively. Apparently, we notice $E\rho$ has a higher level of detail than the $\mu\rho$ attribute. The upper parts of the figures exhibit lower values of the attributes as they correspond to the sandstone presence, whereas the higher values are seen in the lower part, verifying the availability of dolomitic siltstone in this zone. The time slices of $\mu\rho$ and $E\rho$ attributes taken for the Montney formation are illustrated in [Figures 4a and b](#), respectively, the arrows indicating the points where very noticeable information on lithology is clearly seen on the section.

[Figure 3](#) and [Figure 4](#) have illustrated the application of $E\rho$ attribute as lithology indicator. Next, we illustrate the application of $E\rho$ attribute as a significant litho-fluid discriminator. In [Figure 5](#), we illustrate the crossplots of $\kappa\rho - \mu\rho$ and $\kappa\rho - E\rho$. We notice the main trends for the different clusters (in the $\kappa\rho - \mu\rho$ and $\kappa\rho - E\rho$ domains), are more or less the same, however, the separation of the different clusters is much more in the $\kappa\rho - E\rho$ crossplot space than in the $\kappa\rho - \mu\rho$ space. We back project the different clusters onto the seismic sections in [Figure 6](#) and notice that $\kappa\rho - E\rho$ reveals more accurate lithologic information. Upper and lower parts of Nordegg formation are seen holding distinctive characteristic in $\kappa\rho - E\rho$ domain while they are indistinguishable in $\kappa\rho - \mu\rho$ domain. Similar distinctions can be seen for the Fernie and Montney formations.

Conclusions

We have proposed a new attribute ($E\rho$) in the form of a product of Young's modulus and density, which is a good lithology indicator. We describe it as a scaled version of the $\mu\rho$ attribute and illustrate that it intensifies the variation in lithology. This attribute can be derived seismically and have shown that we can determine the brittleness of a formation with it. Clusters in $\kappa\rho - E\rho$ crossplot space corresponding to the litho-fluids are seen to be discriminated better than between similar clusters in the $\kappa\rho - \mu\rho$ space.

Acknowledgements

We thank Arcis Seismic Solutions for encouraging this work and for permission to present these results.

References Cited

Banik, N., K. Adam, and K. Kaseeh, 2010, Young's modulus from point-receiver surface seismic data: SEG Expanded Abstracts, v. 29, p. 2794-2798.

Dabagh, H., Hazim, and S. Alkhafaf, 2011, Comparison of $\kappa\rho$ and $\lambda\rho$ in clastic rocks: A test on two wells with different reservoir-quality stacked sands from West Africa: The Leading Edge, v. 30, p. 986-994.

Goodway, B., T. Chen, and J. Downton, 1997, Improved AVO fluid detection and lithology discrimination using Lamé petrophysical parameters: 67th SEG Annual International Meeting., SEG, p. 183-186.

Katahara, W.K., 2001, Lamé's parameter as a pore-fluid indicator: A rock-physics perspective: SEG Expanded Abstracts, v. 20, p. 326-328.

Russell, B.H., K. Hedlin, F. Hilterman, and L.R. Lines, 2003, Fluid-property discrimination with AVO: A Biot-Gassmann perspective: Geophysics, v. 68, p. 29-39.

Santoso, D., S. Alam, L. Hendraya, S. Alfian, and S. Munadi, 1995, Estimation of limestone reservoir porosity by seismic attribute and AVO analysis: Exploration Geophysics, v. 26, p. 437-443.

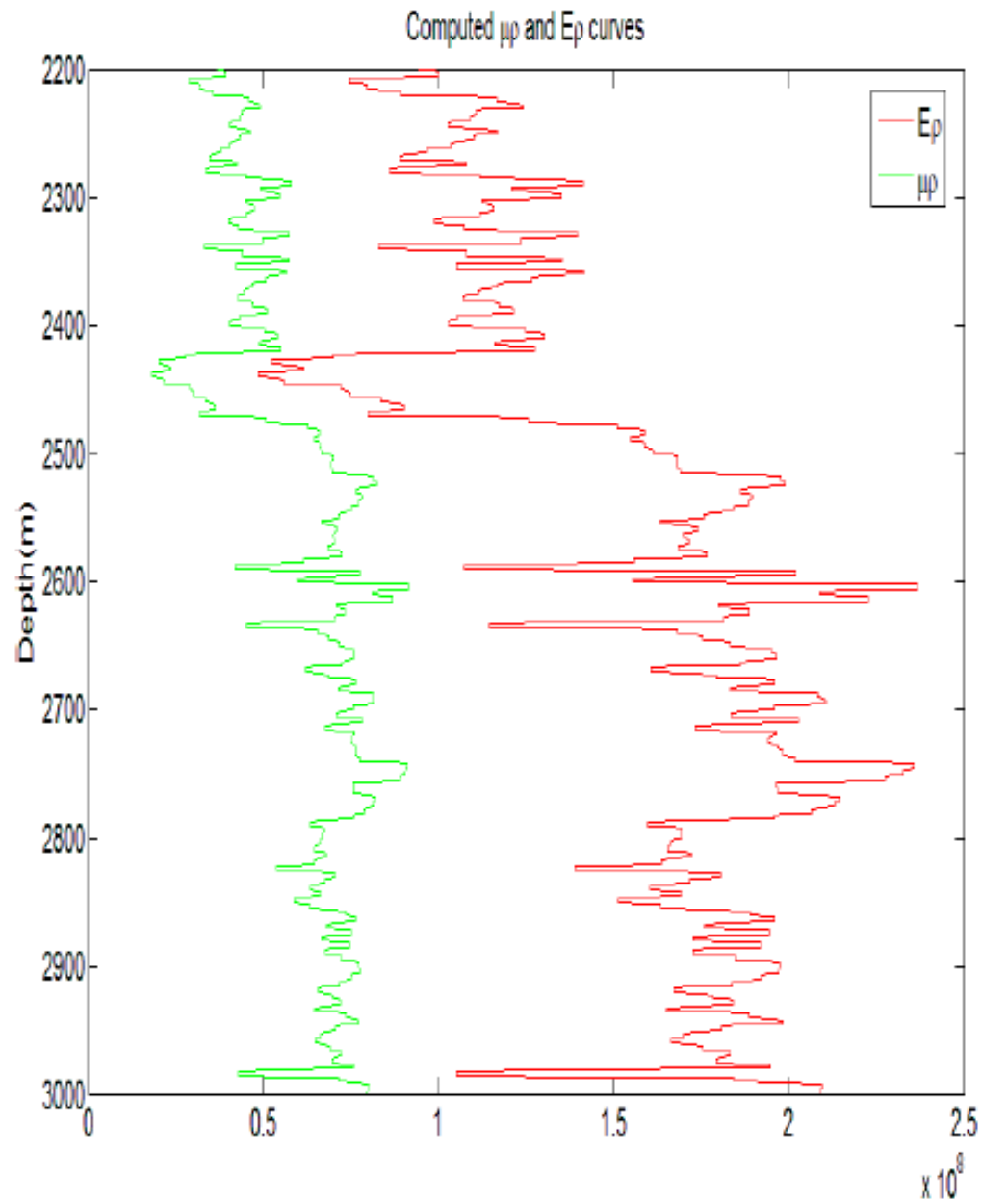


Figure 1. Computed $\mu\rho$ curve (red) plotted against the $E\rho$ curve (green). Notice, the $E\rho$ curve exhibits emphasized lithologic variation than the $\mu\rho$ curve.

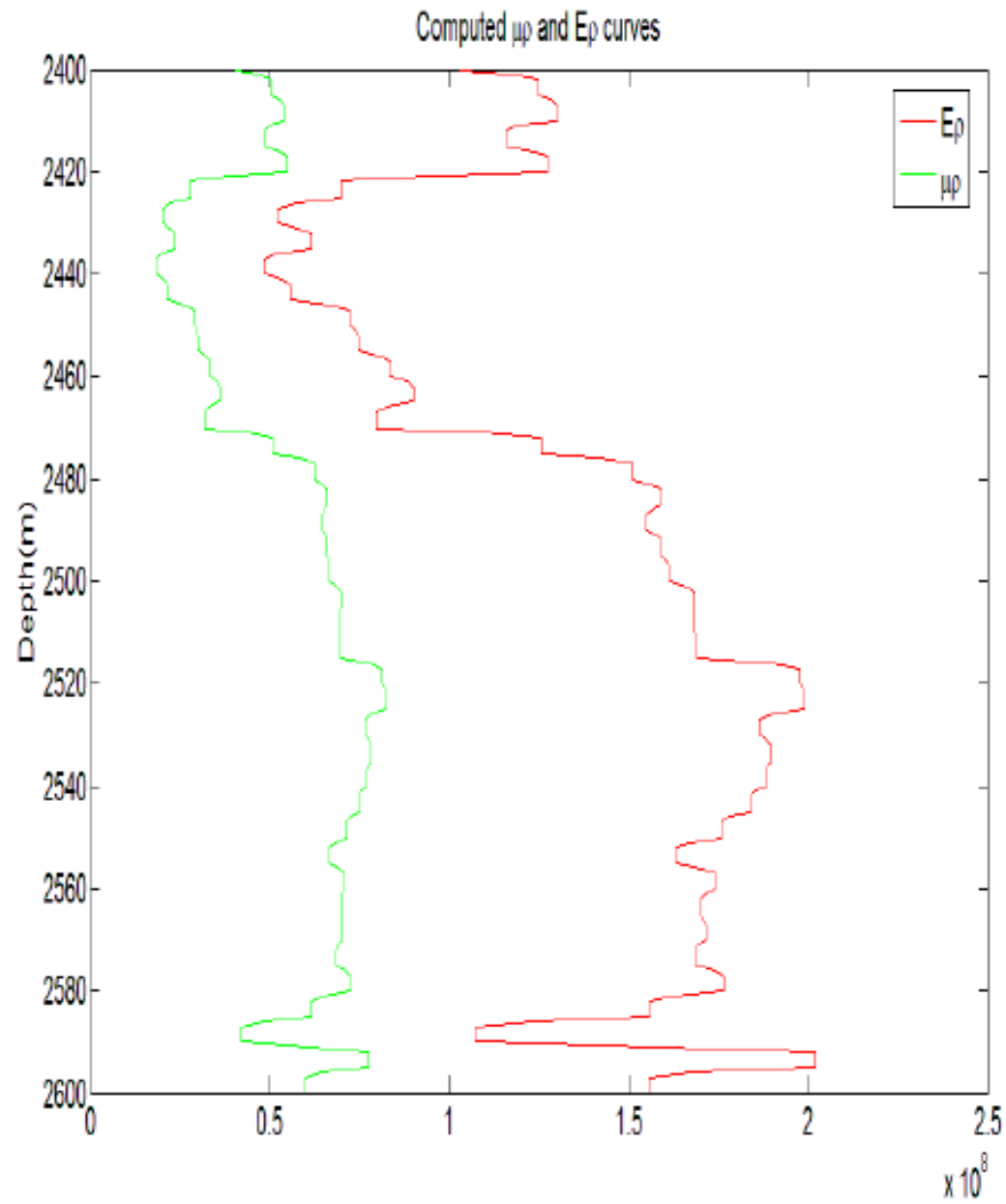


Figure 2. $\mu\rho$ and $E\rho$ curves computed from segmented input logs. On these segmented curves, more emphasized lithologic variation is seen on the $E\rho$ curve than on the $\mu\rho$ curve.

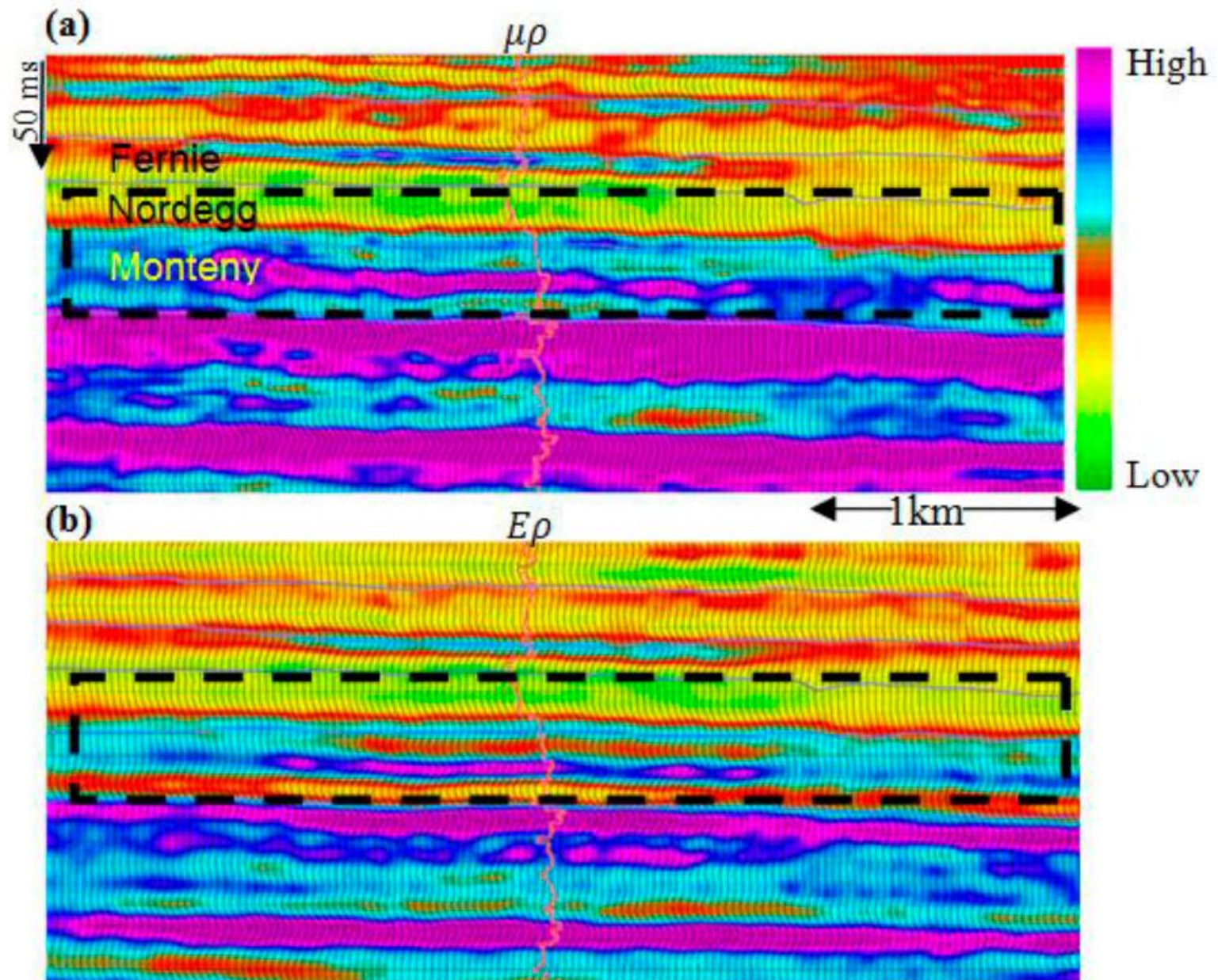


Figure 3. Comparison of (a) $\mu\rho$ section with (b) $E\rho$ section, which illustrates the detailed lithology information seen on the $E\rho$ section compared with the $\mu\rho$, especially in the rectangular highlighted area.

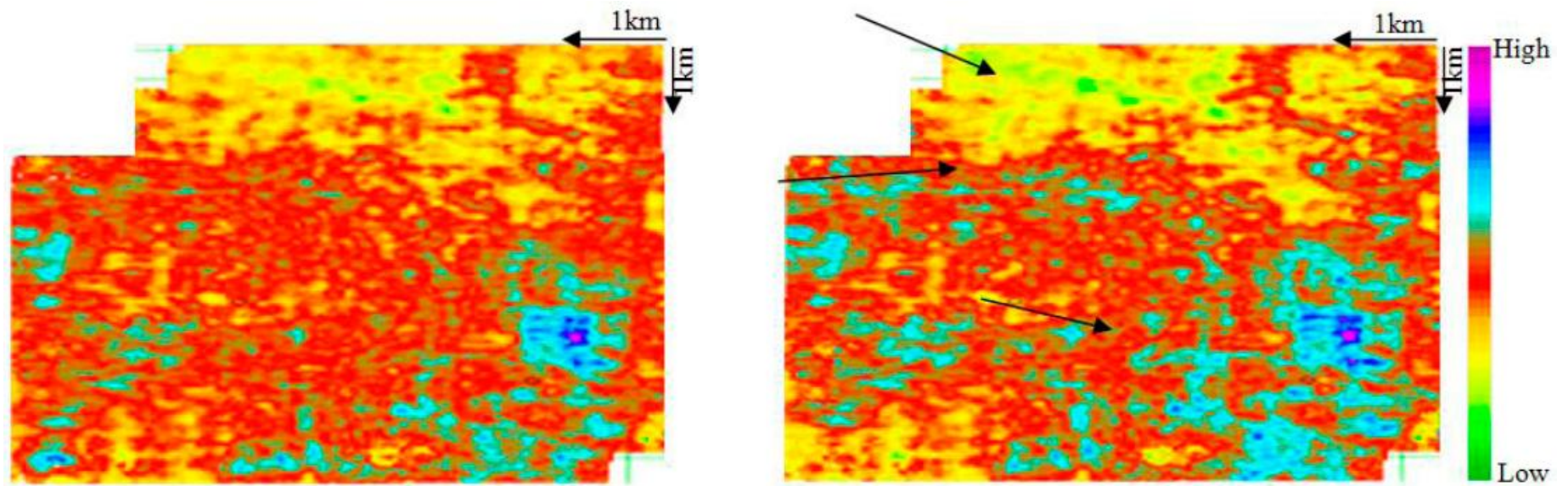
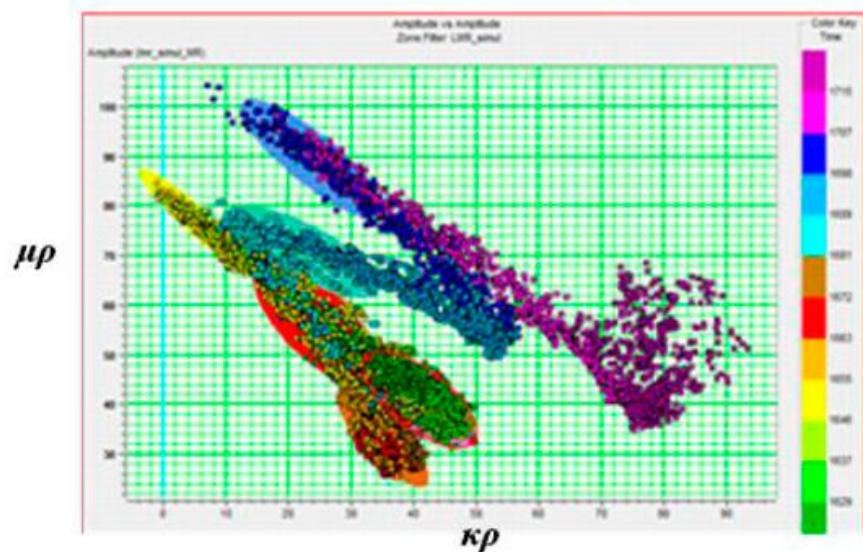


Figure 4. (a) Time slice from the $\mu\rho$ attribute volume taken at the Montney level, (b) equivalent time slice to shown in (a), from the $E\rho$ attribute volume displaying more emphasized detail pertaining to lithology. Arrows indicate the pockets where lithologic information is seen more emphasized than others.

(a)



(b)

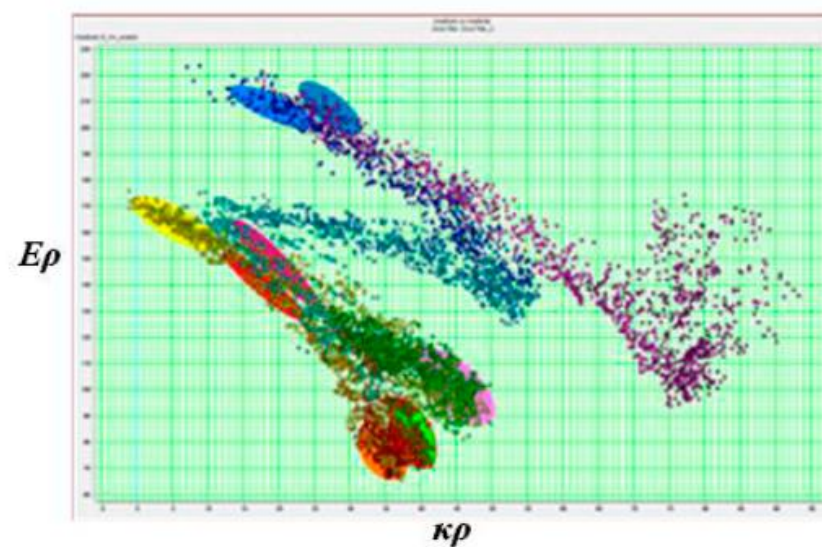
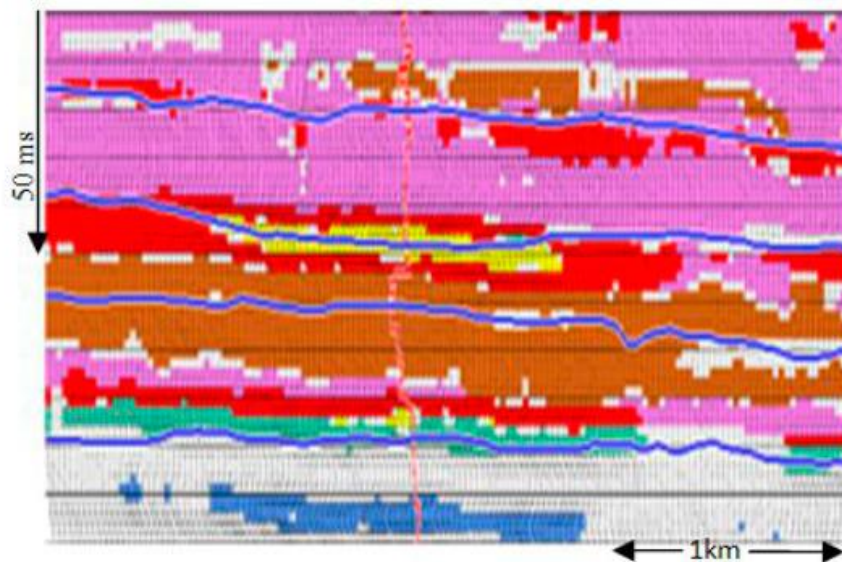


Figure 5. (a) Crossplot of $\kappa\rho$ - $\mu\rho$ with cluster covering the Feni, Nordegg and the Montney formations. Clusters corresponding to these formations are seen separated; (b) Crossplot of $\kappa\rho$ - $E\rho$ with cluster covering the Feni, Nordegg and the Montney formations. Clusters corresponding to these formations are seen much better separated than shown in (a).

(a)



(b)

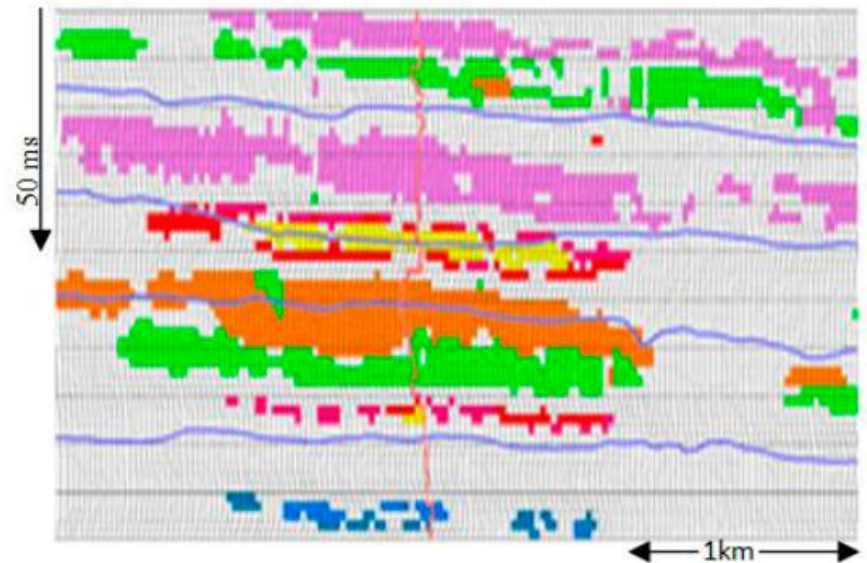


Figure 6. Back projection of cluster points enclosed in polygons as seen in (a) [Figure 5a](#); (b) [Figure 5b](#). Notice that upper and lower part of the Montney formation is distinguishable. Ferni and Nordegg formations are also seen as showing variation within their own zones.